Taylor & Francis
Taylor & Francis Group

RESEARCH PAPER - BASIC SCIENCE

🔓 OPEN ACCESS Check for updates

Vitamin D improves sunburns by increasing autophagy in M2 macrophages

Lopa M. Das[a], Amy M. Binko[a], Zachary P. Traylor[a], Han Peng[b], and Kurt Q. Lu 🆔[a,b,c]

[a]Department of Dermatology, Case Western Reserve University School of Medicine, Cleveland, OH, USA; [b]Department of Dermatology, Northwestern University, Chicago, IL, USA; [c]Department of Dermatology, University Hospitals Cleveland Medical Center, Cleveland, OH, USA

ABSTRACT

Cutaneous inflammation from UV radiation exposure causes epidermal damage, cellular infiltration, and secretion of pro-inflammatory mediators that exacerbate tissue destruction. Recovery is mediated chiefly by anti-inflammatory M2 macrophages that suppress inflammation and augment epidermal regeneration. Vitamin D enables anti-inflammation to promote tissue repair in response to injury. Since vitamin D enhances cellular macroautophagy/autophagy, we investigated the role of autophagy in vitamin D protection of UV-mediated sunburn and inflammation. Using a UV-mediated acute skin injury mouse model, we demonstrate that a single dose of vitamin D resolves injury with sustained inhibition of inflammatory cytokines associated with enhanced autophagy in myeloid anti-inflammatory M2 macs. Increased MAP1LC3B/LC3 expression corroborated with complete autolysosome formation detected by electron microscopy and correlated with degradation of SQSTM1/p62 in the skin following vitamin D treatment. Specifically, pharmacological inhibition of autophagy increased UV-induced apoptosis, suppressed M2 macs recruitment, and prevented vitamin D downregulation of *Tnf* and *Mmp9* in the skin. Furthermore, selective deletion of autophagy in myeloid cells of *atg7* cKO mice abrogated vitamin D-mediated protection and recapitulated UV-induced inflammation. Mechanistically, vitamin D signaling activated M2-autophagy regulators *Klf4*, *Pparg*, and *Arg1*. Lastly, analysis of UV-exposed human skin biopsies detected a similar increase in macrophage autophagy following vitamin D intervention, identifying an essential role for autophagy in vitamin D-mediated protection of skin from UV damage.

Abbreviations: ARG1: arginase 1; ATG7 cKO: autophagy related 7 conditional knockout; HPF: high powered field; KLF4: Kruppel like factor 4; MAP1LC3B/LC3: microtubule-associated protein 1 light chain 3 beta; macs: macrophage; 3-MA: 3-methyladenine; MMP9: matrix metallopeptidase 9; NOS2: nitric oxide synthase 2, inducible; PPARG: peroxisome proliferator activated receptor gamma; SQSTM1/p62: sequestosome 1; TNF: tumor necrosis factor; UV: ultraviolet; VD: vitamin D, 25-hydroxy vitamin D_3; 1,25-VD: 1, 25-dihydroxy vitamin D_3

Introduction

UV (ultraviolet) radiation is a ubiquitous environmental stressor that upon excessive exposure inflicts acute skin damage and initiates a cascade of inflammatory reactions that exacerbate tissue destruction resulting in delayed wound healing [1–3]. We have previously demonstrated in a human clinical study that intervention of experimentally induced sunburn with orally administered cholecalciferol D_3 attenuates skin inflammation by inhibiting *NOS2* (nitric oxide synthase 2, inducible) and *TNF* (tumor necrosis factor). Accelerated skin repair is associated with increased expression of anti-inflammatory M2 macrophage-specific protein ARG1 (arginase 1) [4], however the mechanism of vitamin D mediated protection by dampening of inflammation remains unknown.

Vitamin D, an endocrine hormone that can be obtained from nutrient sources or naturally synthesized in the skin, is thought to confer survival and fitness to cells through modulation of autophagy [5,6]. Autophagy is a cellular protein degradative pathway that mediates turnover of organelles and damaged proteins to maintain homeostasis and is integral in expanding nematode lifespan with congruent effects in mice [7]. More recently autophagy is implicated in playing an immunomodulatory role to counter environmental stressors in chronic inflammation and in models of infection [8–11]. In this study we investigated the role of autophagy in vitamin D mediated regulation of cutaneous inflammatory responses from an experimentally-induced sunburn. Inhibition of inflammation is associated with upregulated expression of anti-inflammatory enzyme *Arg1*, downmodulation of competitor enzyme *Nos2*, and expansion of anti-inflammatory M2 macs [12]. Since NOS2 activation is antagonistic to autophagy [13], we sought to understand whether vitamin D regulates autophagy to mediate its anti-inflammatory effects in the skin.

Our results show for the first time that vitamin D suppressed skin inflammation and accelerated tissue recovery by upregulating autophagy, especially within MRC1/CD206+ M2 macs. Induction of autophagy is associated with expression of *Klf4* and activation of the vitamin D receptor and *Pparg* pathway. Thus our results identify vitamin D-induced autophagy as a potential therapeutic option for treating UV-induced acute

Results

Attenuation of skin inflammation following UV exposure by vitamin D

Given the purported immunomodulatory effects of vitamin D we sought to determine whether vitamin D can alleviate acute inflammation following injury from a severe sunburn. Mice were irradiated with an erythemogenic dose of UV radiation (100 mJ/cm^2) in an established protocol known to cause epidermal damage with induction of dermal inflammation composed predominantly of monocytes and macrophages [14,15]. As expected, on day 2 post UV exposure,

pronounced erythema and inflammation was observed on the dorsal back compared to no UV control animals (Figure S1). Histopathological analysis revealed massive cellular infiltration in the dermis with dermal edema (Figure 1(a)). On days 3 and 5 post-irradiation respectively, skin wounds were progressively worsened with complete erosion of the epidermis, persistence of edema, and disruption of subcutaneous fat (Figure 1(b,c)). In contrast, intervention with a single intraperitoneal (i.p.) injection of vitamin D in the 25-hydroxy vitamin D$_3$ form 1 h after UV exposure delayed skin inflammation, arrested wound progression and accelerated wound repair by day 5 (Figure 1(d–f)). There was muted dermal injury and epidermal erosion by day 3 with preservation of dermal and epidermal integrity (Figure 1(e)). The UV-induced wound area (mm^2) was reduced most dramatically by vitamin D treatment on day 4 (Figure1(g)). Lastly, there
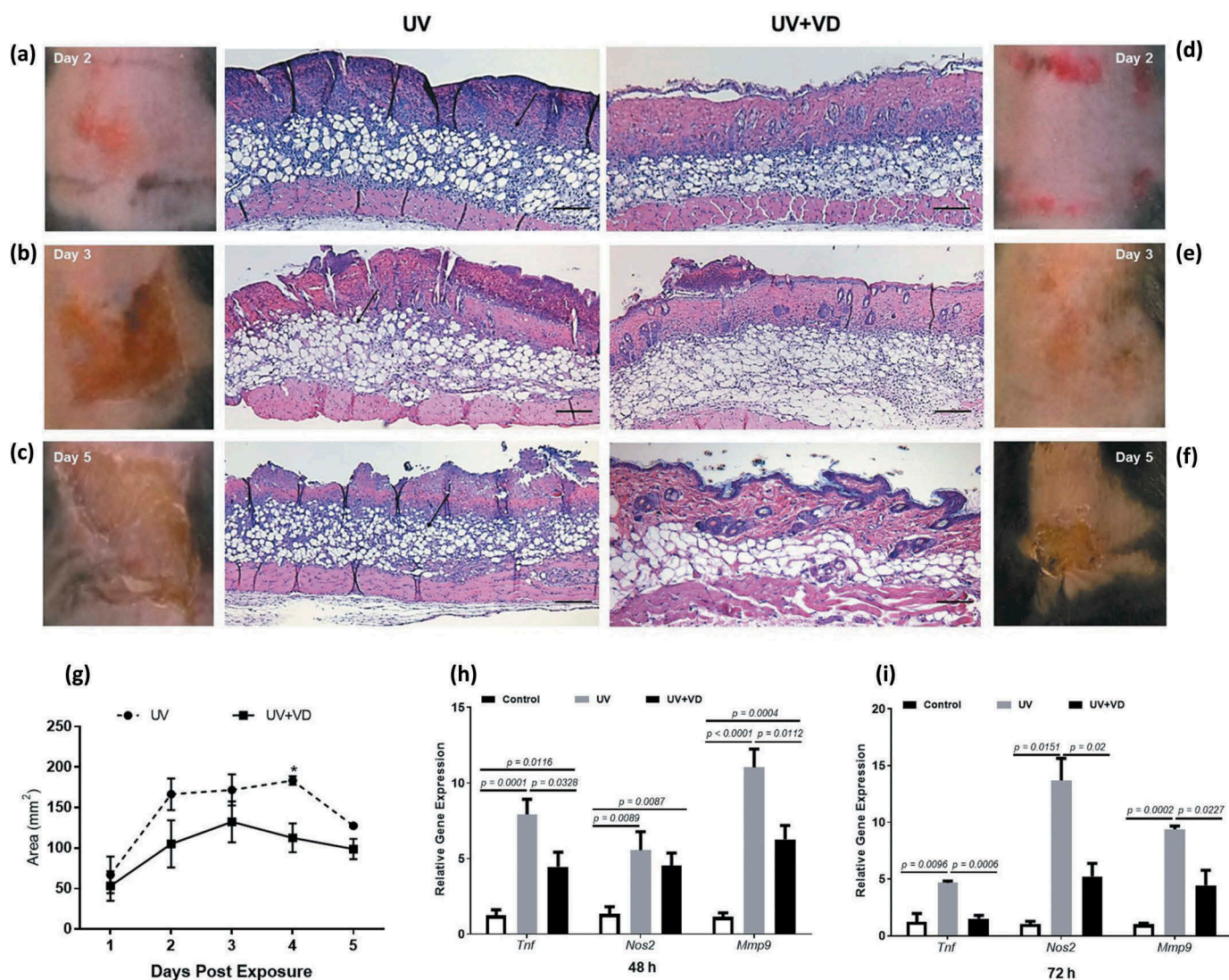

Figure 1. Vitamin D protects from UV-mediated skin inflammation. C57BL/6 mice were exposed to 100 mJ/cm^2 UV radiation 48 h following shaving and hair depilation from their dorsal side. 1 h following UV, mice were treated with vitamin D (VD), administered i.p. At indicated time points skin was harvested for histology. (a-f) Wound and parallel histopathology images of UV exposed skin (a-c) and following treatment with VD (d-f) at days 2, 3, and 5 post irradiation. Skin was excised post mortem, sectioned and stained with hematoxylin and eosin for histopathological evaluation. Scale bar: 100 μm. (g) Quantification of the area of redness at the site of UV exposure, p = 0.04 at day 4 post UV using ImageJ software, (n = 4 for UV and n = 5 for UV+VD). (h and i) Evaluation of inflammatory markers *Tnf, Nos2 and Mmp9* by qPCR using RNA isolated from skin at 48 h and 72 h following UV exposure (n = 6 for all groups at 48 h, n = 3 for all groups at 72 h, p<0.005 using a paired t-test).

was significant and sustained down-regulation of skin inflammatory factors including *Nos2, Tnf,* and *Mmp9* in the vitamin D treatment group (Figure 1(h,i)).

Macrophage-specific autophagy is enhanced by vitamin D

It is known that vitamin D promotes autophagy, therefore we next examined whether vitamin D upregulates autophagy in the tissue infiltrating macrophages of UV-irradiated skin. Immunofluorescence microscopy for detection of cellular autophagy marker LC3 revealed that as a stressor signal, UV exposure alone induced autophagy compared to control (Figure 2(a,b)). Treatment with vitamin D following UV exposure further enhanced LC3 expression, especially in dermal infiltrating ADGRE1$^+$/F4/80$^+$ (adhesion G protein-coupled receptor E1) macrophages (Figure 2(c)). This

observation was completely abrogated in all experimental treatment conditions when animals were pretreated i.p. with 3-MA (3-methyl adenine), a pharmacological inhibitor of autophagy (Figure 2(d–f)). Functionally we evaluated the dependence of vitamin D and autophagy on the expression of *Pparg*, an anti-inflammatory nuclear receptor, and pro-inflammatory cytokines *Tnf* and *Mmp9*. Compared to UV, treatment with vitamin D restored *Pparg* back to baseline levels (Figure 2(g)) that was partially dependent on autophagy. Vitamin D suppressive effect on pro-inflammatory cytokines (Figure 2(h,i)) was observed to be heavily dependent on autophagy resulting in significant upregulation of *Tnf* and *Mmp9* in 3-MA treated animals (Figure 2(g,h)). Taken together, these results demonstrate that a single treatment with vitamin D mediates anti-inflammation in the skin via modulation of autophagy in dermally infiltrated myeloid macrophages.
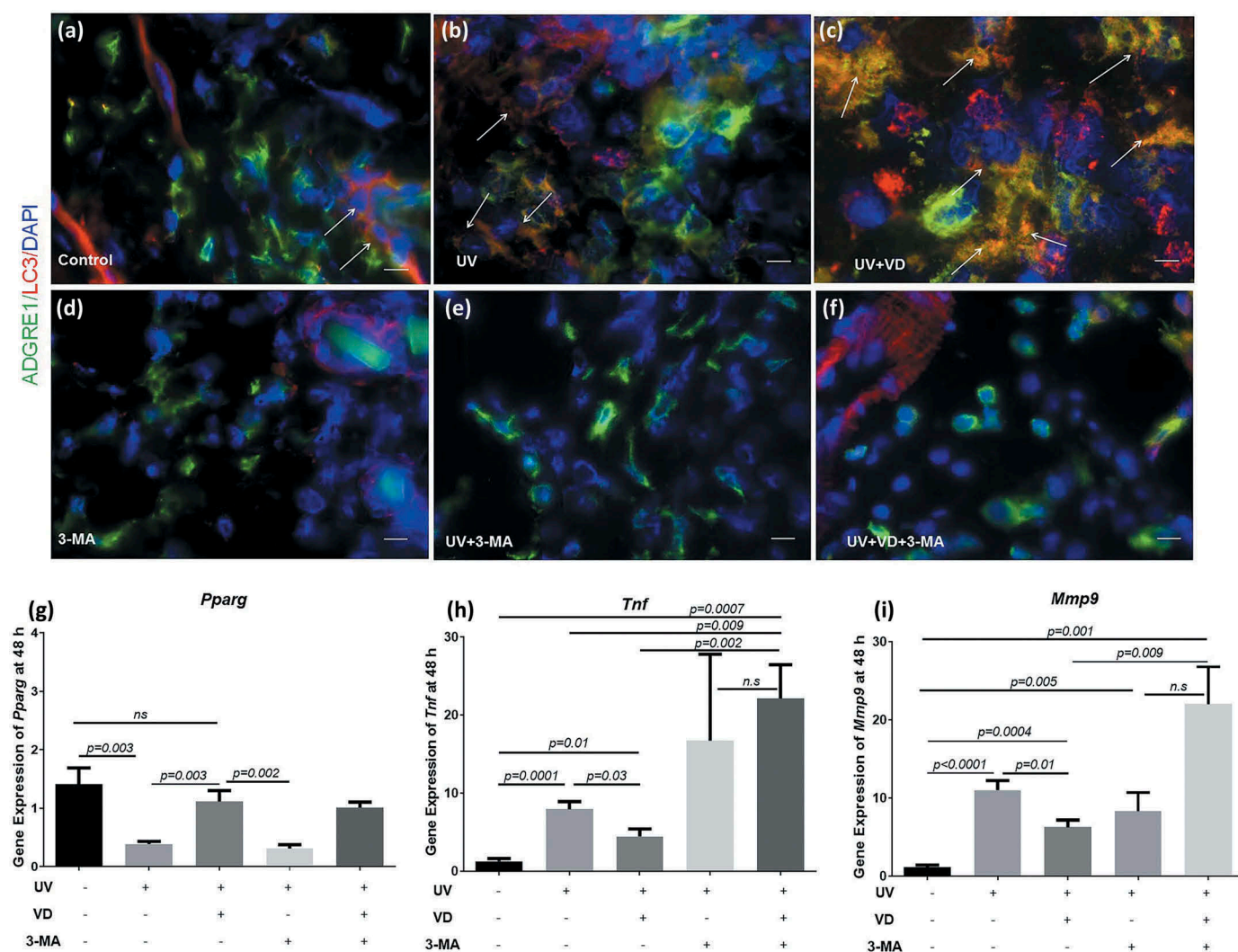

Figure 2. Vitamin D enhances macrophage-specific autophagy and diminishes inflammation in an autophagy dependent manner. Skin sections were subject to (a-f) confocal microscopy at 72 h and (g-i) real time PCR at 48 h post UV. (a-f) Representative images of skin tissue sections stained for immunofluorescent detection of ADGRE1 (green), LC3 (red), (yellow, indicative of co-localization, is marked with arrows), and DAPI (blue). Tissue gene expression of anti-inflammatory mediator (g) *Pparg*, and pro-inflammatory mediators (h) *Tnf*, and (i) *Mmp9* were quantified following blockade of autophagy by pharmacological inhibitor 3-MA, (p ≤ 0.03). For *Tnf* and *Mmp9*, n = 6 for all groups except UV+3-MA n = 4, for *Pparg* n = 6 for all groups except control n = 5 and UV+VD+3-MA n = 10. Scale bar: 20 μm.

Autophagic flux in macrophages of UV exposed mouse skin is augmented by vitamin D

Next we evaluated the expression levels of LC3 and SQSTM1 in mouse skin tissue 48 h following UV exposure as an indicator of autophagy processing. A single treatment with vitamin D increased tissue expression of LC3II compared to UV, control, and other treatment conditions. This was accompanied by a dramatic decrease in SQSTM1 expression, indicative of degradation of protein levels and complete processing of autophagy following treatment with vitamin D. To demonstrate regulation of autophagy, LC3II and SQSTM1 levels were assessed following inhibition of autophagy with 3-MA. Reduced LC3II expression and increased SQSTM1 levels were noted with 3-MA that could not be reversed fully even after treatment with vitamin D (Figure 3(a,b)). To visualize incidence and extent of autophagic puncta specifically in macrophages, skin cells were isolated from whole skin ex vivo and placed on coverslips to detect occurrence of autophagy through expression of LC3. Representative fluorescent microscopic images revealed a 5-fold increase in LC3 puncta percent positivity (red) in ADGRE1^{+} (green) macrophages isolated from vitamin D treated mice compared to UV alone (Figure 3(c–e)) with quantitative analysis across samples showing a significant 1.5-fold increase in percent positivity (Figure 3(f)).

To further validate the immunofluorescent microscopic data, autophagic activity was imaged using transmission electron microscopy (TEM). Ultrastructural examination of macrophages revealed presence of autophagosomes following UV exposure compared to no UV control and UV+3-MA
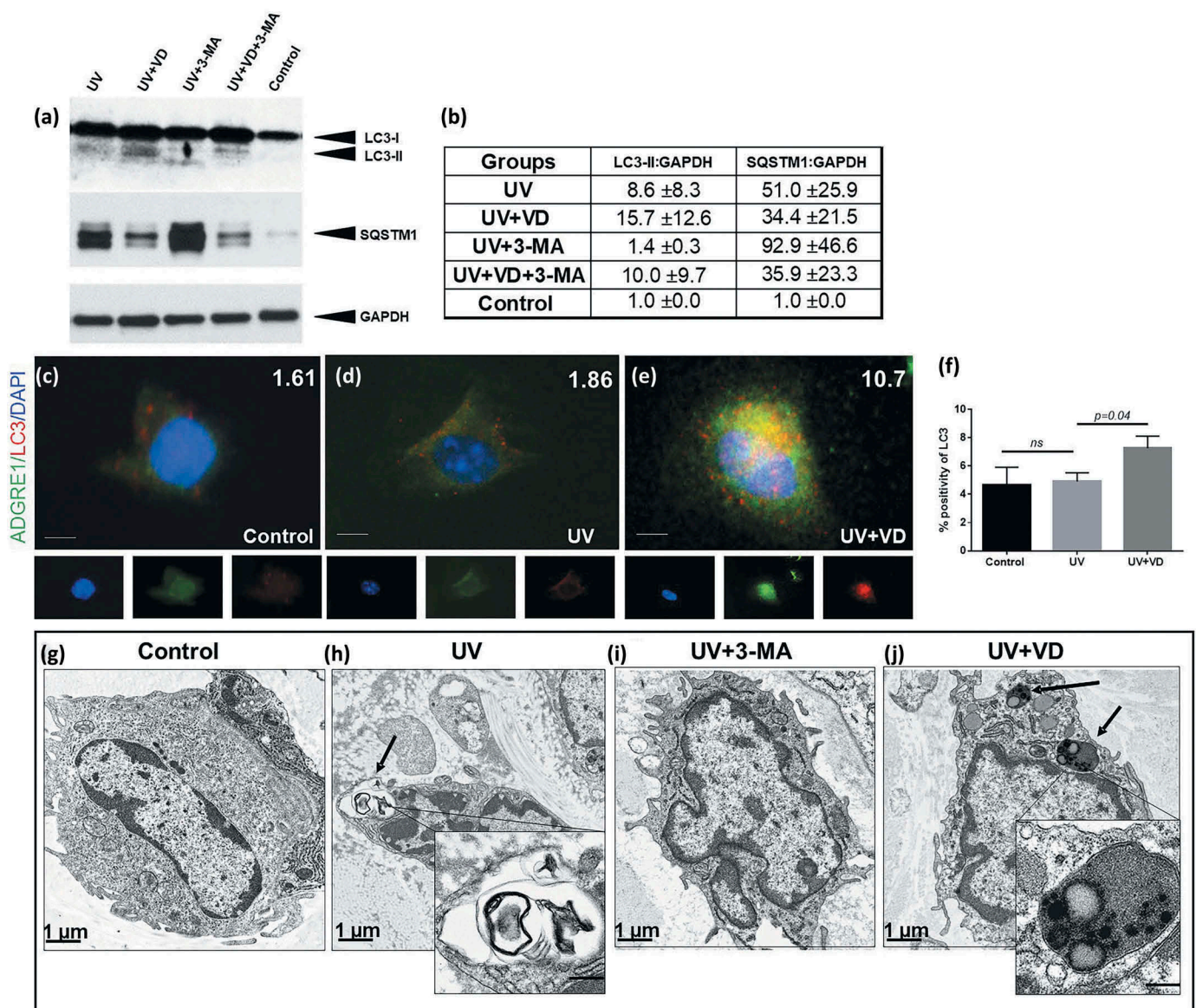

Figure 3. Vitamin D augments autophagic flux in macrophages of UV exposed mouse skin. Skin was harvested 48 h post UV and (a) tissue sections homogenized to prepare protein lysates for detection of LC3-I, LC3-II and SQSTM1 by immunoblot analysis, and (b) quantified by densitometry, (c-e) digested to obtain cells for ex vivo staining of control, UV and UV+VD, for detection of ADGRE1 (green), LC3 (red), and DAPI (blue). Scale bar: 10 μm. Number on the images represent percent positivity of LC3^{+} puncta quantified using the scoring application module of MetaMorph. (f) Graphical representation of quantitated puncta positivity (n = 8 for control and UV, n = 10 for UV+VD). (g-j) Transmission electron microscopy images of skin tissue that were fixed and sectioned for detection of macrophage autophagic activity (indicated by arrows, inset) in (g) control, (h) UV, (i) UV+3-MA and (j) UV+VD treated mice. Scale bar: 1 μm.

treated animals (Figure 3(g–j)). However formation of complete autolysosomal bodies with cellular inclusions was most evident in the vitamin D tissue compared to the UV group (Figure 3(h,j)). Together these findings confirmed the differential effect of vitamin D on dermally infiltrated myeloid macrophages to up regulate autophagy processing and completion in cutaneous tissue.

Vitamin D restored anti-inflammatory M2 macrophages in an autophagy-dependent manner

Next we sought to determine whether vitamin D intervention alters the macrophage infiltrates in this UV model. Flow cytometric analysis of whole skin cell isolates demonstrate a homeostatic distribution of macrophages into two distinct populations – PTPRC$^+$ ADGRE1$^+$ LY6C$^+$ MRC1/CD206$^-$ M1 macs and PTPRC$^+$ ADGRE1$^+$ LY6C$^-$ MRC1$^+$ M2 macs (Figure 4(a–e)). At baseline non-inflamed control skin revealed an abundance of M2 macs compared to inflammatory M1 macs, possibly to maintain quiescence and homeostasis (Figure 4(a)). UV exposed animals demonstrated a shift towards an increased inflammatory M1 population, significantly altering the ratio of M2 macs to M1 macs in the skin (Figure 4(b,f)). Intervention with vitamin D restored that distribution to relative abundance of M2 macs and reduced M1 macs in the skin compared to UV alone (Figure 4(c,f)). Furthermore, in vivo inhibition of autophagy with 3-MA disrupted the effect of vitamin D, resulting in a distribution that shifted towards M1 macs (Figure 4(d,e)).

We next examined the macrophage populations as a percentage of all skin cells. As expected, UV exposure induced inflammation resulting in a significant increase of ADGRE1$^+$ macrophages across all experimental conditions compared to control, with no significant differences between the treatment groups (Figure 4(g)). Vitamin D intervention did not diminish the total percentage of macrophages in the skin but rather it decreased the percentage of M1 macs and increased the percentage of M2 macs (Figure 4(h,i)). Interestingly, inhibition with 3-MA treatment did not alter the M1 mac population (Figure 4(h), bar 3 vs. bar 5), rather it significantly diminished the increase of M2 macs observed with vitamin D (Figure 4(i), bar 3 vs. bar 5). These data demonstrate that while vitamin D has differential effects on macrophage populations, the effect on the M2 macs subset is autophagy dependent.

Selective upregulation of LC3 expression in MRC1$^+$ M2 macrophages after treatment with vitamin D

Next we sought to characterize expression levels of LC3 in M1 and M2 macs. Evaluation of MFI (mean fluorescence intensity) by flow analysis demonstrated the highest values LC3 MFI in M2 macs in the vitamin D treatment group, absent with 3-MA treatment (Figure 5(a–e)). Additionally, skin sections were stained to detect and co-localize LC3 with M2 marker MRC1. Vitamin D treatment significantly increased LC3$^+$ MRC1$^+$ cells in the dermis compared to UV only and control (Figure 5(f-h)). Inhibition of
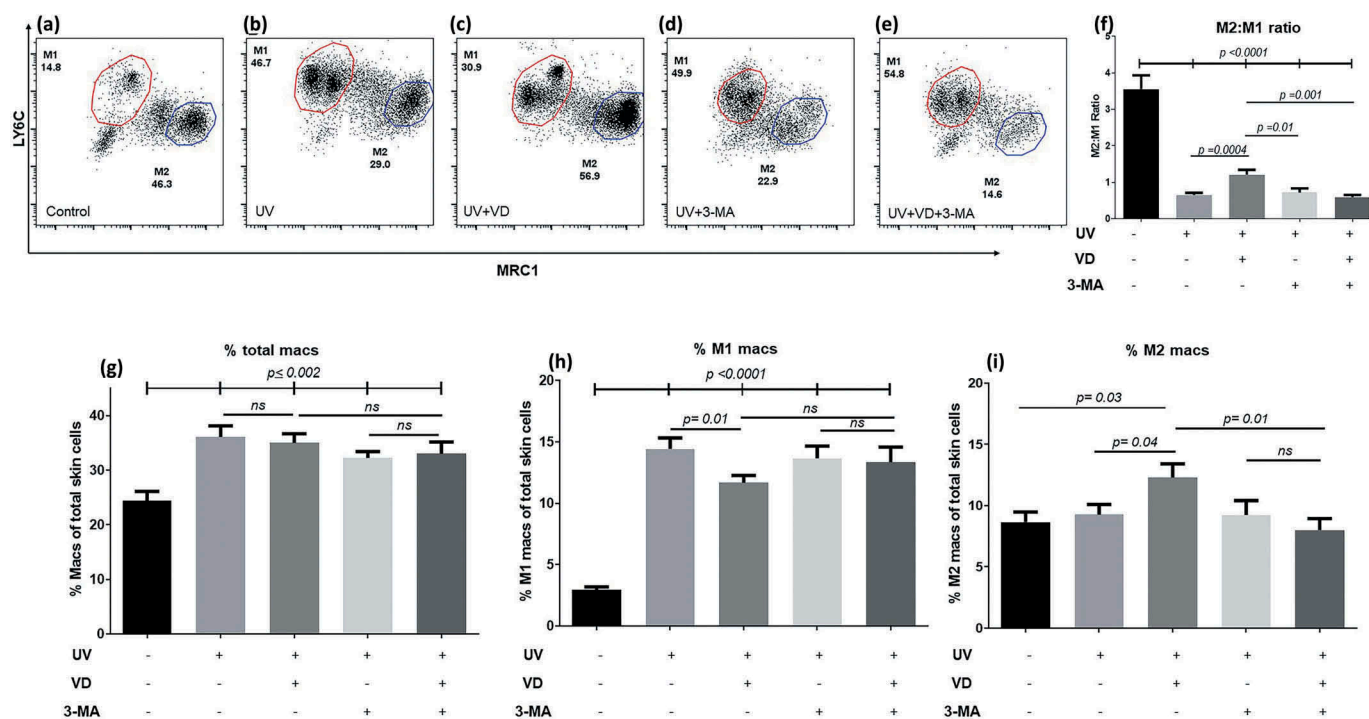

Figure 4. Vitamin D repopulates M2 macrophages in the inflamed skin in an autophagy-dependent manner. Cells were harvested from control and irradiated skin, 48 h post exposure, in presence or absence of VD and/or 3-MA for detection of PTPRC (myeloid), ADGRE1 (macrophage), LY6C (M1), and MRC1 (M2). Representative dot plots indicate distribution of PTPRC$^+$ ADGRE1$^+$ cells into 2 separate populations – LY6C$^+$ MRC1$^-$ (M1) and LY6C$^-$ MRC1$^+$ (M2) in (a) control, (b) UV, (c) UV+VD, (d) UV+3-MA, (e) UV+VD+3-MA and graphical representation of (f) ratio of M2 to M1 macrophages. (g–i) Quantification of skin infiltrating myeloid macrophages to include (g) total percent myeloid PTPRC$^+$ ADGRE1$^+$ macrophages, (h) percent PTPRC$^+$ LY6C$^+$ or M1 macrophages and (i) percent PTPRC$^+$ ADGRE1$^+$ MRC1$^+$ or M2 macrophages, (n = 26 for control, n = 37 for UV, n = 45 for UV+VD, n = 22 for UV+3-MA, and n = 23 for UV+VD+3-MA), (p ≤ 0.04).
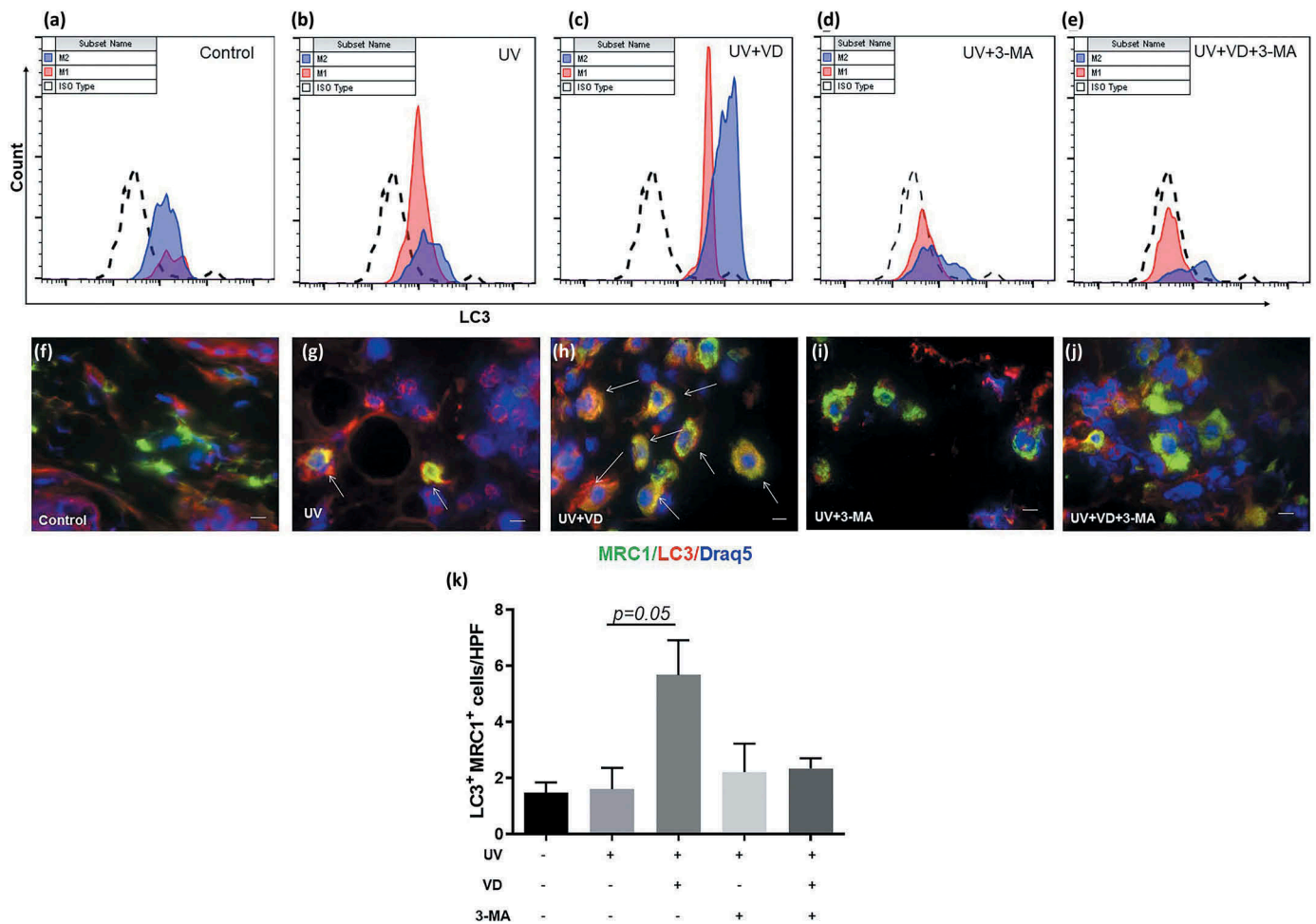
Figure 5. LC3 expression is selectively upregulated in MRC1+ M2 macrophages after treatment with vitamin D. (a–e) Cells were harvested from UV-irradiated skin of all treatment groups. Cells were stained for flow cytometric analysis of PTPRC (myeloid), ADGRE1 (macrophage), LY6C (M1), MRC1 (M2), and LC3 (autophagy). Histograms showing LC3 counts and MFI within M1 and M2 macrophage populations in (a) control, (b) UV, (c) UV+VD, (d) UV+3-MA, and (e) UV+VD+3-MA. Skin tissue sections were subject to immunofluorescent staining to detect LC3 expression in MRC1+ M2 macrophages. Representative immunofluorescence images of mouse skin tissue to detect co-localization of MRC1 (green), LC3 (red), and DAPI (blue) in (f) control, (g) UV, (h) UV+VD, (i) UV+3-MA, and (j) UV+VD+3-MA. Arrows point to colocalization. (k) Quantitative representation of MRC1+ LC3+ cells, $p \leq 0.05$, (n = 3 for all groups). Scale bar: 20 µm.

autophagy by 3-MA reduced LC3 expression and reduced the number of MRC1+ cells despite treatment with vitamin D (Figure 5(i,j)). Quantification of LC3+ MRC1+cells per high power field (HPF) confirmed a significant increase in autophagy in MRC1+ macrophages following vitamin D treatment (Figure 5(k)). Furthermore, staining for ARG1, an intracellular enzyme that manipulates arginine from being utilized by NOS2 and an M2 marker of anti-inflammatory macrophages, was shown to be selectively upregulated on MRC1+ macrophages in the deep dermis of vitamin D treated mice (Figure S2). Together these data suggest that the phenotype of macrophages populating the UV-inflamed skin is potentially linked to autophagy levels and modulated by vitamin D to achieve protection from inflammation-induced cutaneous tissue damage.
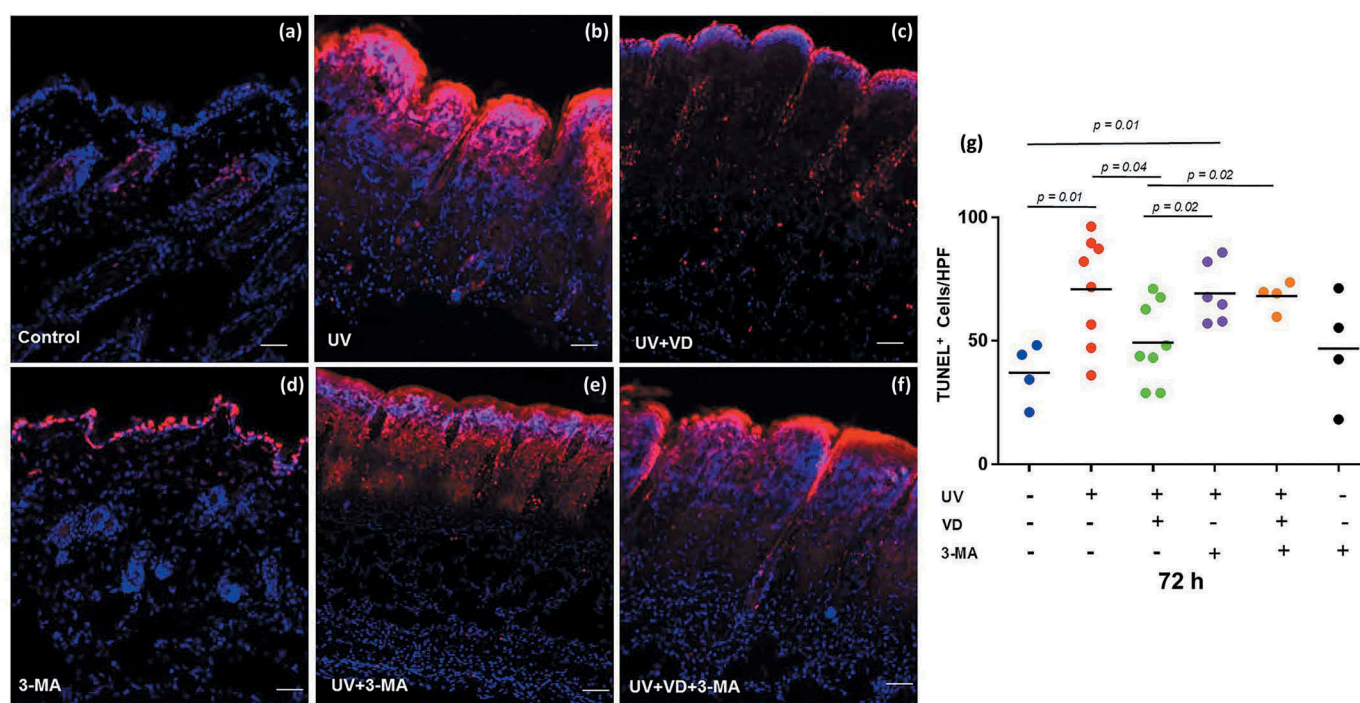
Protection from UV-induced apoptosis in an autophagy-dependent manner by vitamin D

To determine and quantify the extent of cutaneous tissue damage sustained by animals in the UV model, skin sections

were subject to TUNEL assay to evaluate cell death caused by UV-mediated apoptosis. UV exposure inflicted massive cellular apoptosis that is dramatically curbed by vitamin D treatment with significant protection from UV-induced apoptotic cell death compared to control (Figure 6(a-c)). Inhibiting autophagy by 3-MA markedly exacerbated UV-induced tissue damage illustrated by massive epidermal and dermal apoptosis (Figure 6(e)), little of which could be reversed with vitamin D (Figure 6(f)). Cellular apoptosis in tissue was quantified by counting TUNEL+ cells per HPF (Figure 6(g)). Collectively, these data strongly suggest that vitamin D confers protection from UV-mediated cell death and tissue damage, an effect that is dependent on functional autophagy.

Selective depletion of autophagy in myeloid cells impaired the ability of vitamin D to attenuate inflammation

To further confirm the involvement of macrophage autophagy in vitamin D protection against UV-mediated damage, we

TUNEL (apoptotic cell nuclei) /DAPI/Merge of TUNEL and DAPI

Figure 6. Vitamin D protects mice from UV induced apoptosis in an autophagy dependent manner. Skin tissue was harvested from mice 72 h following UV exposure and subject to TUNEL staining to evaluate cellular apoptosis. Representative images of TUNEL+ cells in (a) control, (b) UV and (c) UV+VD mice compared with (d) 3-MA, (e) UV+3-MA, and (f) UV+VD+3-MA mice treated with 3-MA. (g) Quantitation of TUNEL+ cells within affected skin tissue, p ≤ 0.04, (n = 4 for control, UV+3-MA, and UV+VD+3-MA, n = 8 for UV and UV+VD, and n = 6 for 3-MA). Scale bar: 100 μm.

recapitulated the UV model in myeloid-specific *atg7* deficient (*Lyz2/LysM^{Cre} Cre-atg7$^{fl/fl}$*, designated *atg7* cKO) mice [16]. Overall, a less pronounced phenotype was observed in both the *atg7* cKO and the littermates following UV exposure with mild visible skin redness and wound formation (data not shown). However, the histopathology confirmed that UV exposure resulted in marked tissue damage. Vitamin D did not rescue animals from UV induced damage and inflammation in *atg7* cKO mice. We observed comparable dermal necrosis and edema in both the UV and UV plus vitamin D treatment groups (Figure S3A-C). In contrast, littermate control mice demonstrated a response to vitamin D treatment with preservation of epidermal and dermal integrity (Figure S3D-F). Similarly, a representative image by TUNEL assay supported the pattern observed with the histologic images (Figure S4).

Characterization of dermally infiltrated cells following UV exposure revealed that *atg7* cKO mice and littermate controls have abundance of M2 macs under homeostatic conditions (Figure 7(a)). Similar to the response in wild-type mice, UV exposure triggered a large influx of M1 macs into the skin (Figure 7(b)). However, treatment of *atg7* cKO mice with vitamin D did not restore the M2 macs observed with the littermates and with wild-type controls (Figure 7(c)). The cumulative data demonstrated an M2:M1 ratio that remained comparable with and without vitamin D in the *atg7* cKO mice (Figure 7(d)). The littermate controls demonstrated a modest but significant 2-fold increase in M2:M1 ratio relative to UV alone. Further examination of the macrophage subsets as a percentage of all

skin cells revealed that the percent of M1 and M2 macs were comparable between control *atg7* and control littermate groups (Figure S5A,B). The striking observation was that vitamin D exerted no effect on the M1 macs of *atg7* cKO and littermate mice following UV exposure. However, vitamin D significantly expanded M2 macs only in the littermates with no effect on the *atg7* cKO M2 macs (Figure 7(e)). The data recapitulated our experiments using 3-MA in wild-type mice, supporting the observation that the effect of vitamin D on the M2 macs subset is autophagy dependent. Overall these data confirm that autophagy induction in myeloid macrophages is critical to facilitate vitamin D -mediated expansion of anti-inflammatory macrophages and to promote cell survival.

Vitamin D-enhanced autophagy promotes macrophage polarization via activation of KLF4-PPARG pathway

To establish a link between vitamin D-enhanced autophagy and M2 macs polarization, *in vitro* studies were performed with bone-marrow-derived macrophages (BMDMs). We first determined whether macrophage subsets have a differential response to vitamin D by stimulating BMDMs for gene expression levels of *Vdr* (vitamin D receptor). Stimulation of BMDMs with M1 activators IFNG/IFNγ (interferon gamma) and LPS or M2 activator IL4 (interleukin 4) alone did not result in increased expression of *Vdr* (Figure 8(a)). However, when combined with vitamin D, stimulation with IL4 resulted in a synergistic 14-fold increase in *Vdr* expression with only a modest but significant increase with vitamin D and M1
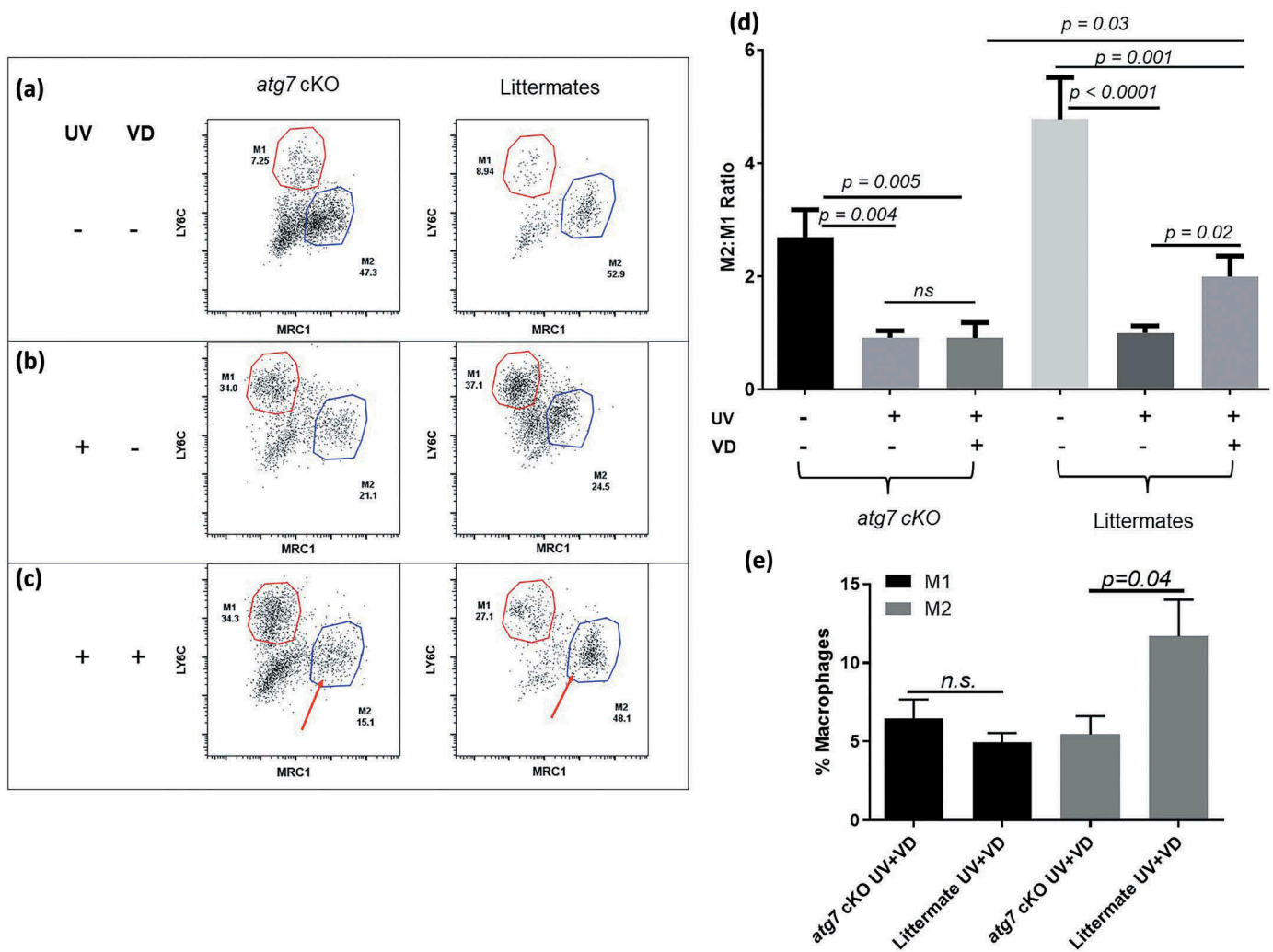
Figure 7. Ablation of autophagy in myeloid cells depletes M2 macrophages and reduces M2:M1 ratio. Skin cells from myeloid autophagy-deficient (*atg7* cKO) mice were harvested for flow cytometric analysis of PTPRC (myeloid), ADGRE1 (macrophage), LY6C (M1), and MRC1 (M2). Representative plots illustrate the distribution of PTPRC$^+$ ADGRE1+ cells into LY6C$^+$ MRC1$^-$ (M1) and LY6C$^-$ MRC1$^+$ (M2) macrophage populations in *atg7* cKO and littermates in groups (a) control, (b) UV, and (c) UV +VD. Arrows indicate absence of MRC1$^+$ M2 macs in VD-treated *atg7* cKO compared to M2 macs restored in VD-treated littermate mice. (d) Quantitation of M2 to M1 ratio in *atg7* cKO and littermates. For *atg7* cKO n = 14 for control, n = 11 for UV, n = 12 for UV+VD, littermates n = 13 for control and UV, and n = 16 for UV+VD. Number on each plot is its M2:M1 ratio ± sem, p<0.03. (e) Quantitation of percent M1 and M2 macs comparing *atg7* cKO and littermate mice treated with UV+VD, (p = 0.04).

stimulation. These results supported our *in vivo* observation that vitamin D treatment leads to expansion of M2 macs and have less effects on M1 macs. Next we evaluated vitamin D and M2 stimulation for M2 hallmark genes. Recently, KLF4, a zinc finger molecule, was demonstrated to be a transcriptional regulator of autophagy critical for promoting cell survival [7]. Interestingly, KLF4 is also established as an important factor in the differentiation of macrophages to M2 macs [17]. When combined, stimulation of BMDM with vitamin D and IL4 resulted in an early and transient activation of *Klf4* (Figure 8(b)). At subsequent time points we observed significant increases of other M2-related genes, *Pparg* and *Arg1* (Figure 8(c,d)). Treatment with vitamin D restored M1-suppressed *Pparg* levels back to baseline value, a pattern reminiscent of *in vivo* restoration of UV-suppressed *Pparg* observed in skin samples of vitamin D treated mice (Figure 2(g)). These observations were specific to M2 activation combined with vitamin D and were not activated by M1

stimulation, which induced the prototypical M1 marker *Cd86* (Figure 8(e)). Together these findings support a role for vitamin D in early induction of *Klf4*, functioning both as an autophagy and M2 transcriptional regulator, to promote M2 macrophage expansion and polarization.

Vitamin D protection from UV-mediated sunburn in human skin is associated with enhanced macrophage specific autophagy

Lastly, to confirm that autophagy is induced and enhanced by vitamin D in humans, skin specimens were obtained from our published double-blinded placebo-controlled clinical pilot study. In this study, each subject's right arm and left arm represented paired-controlled samples for analysis [4]. The paired skin biopsies were from healthy subjects given a single high dose of oral vitamin D or placebo following experimentally induced sunburn. Compared to no treatment,
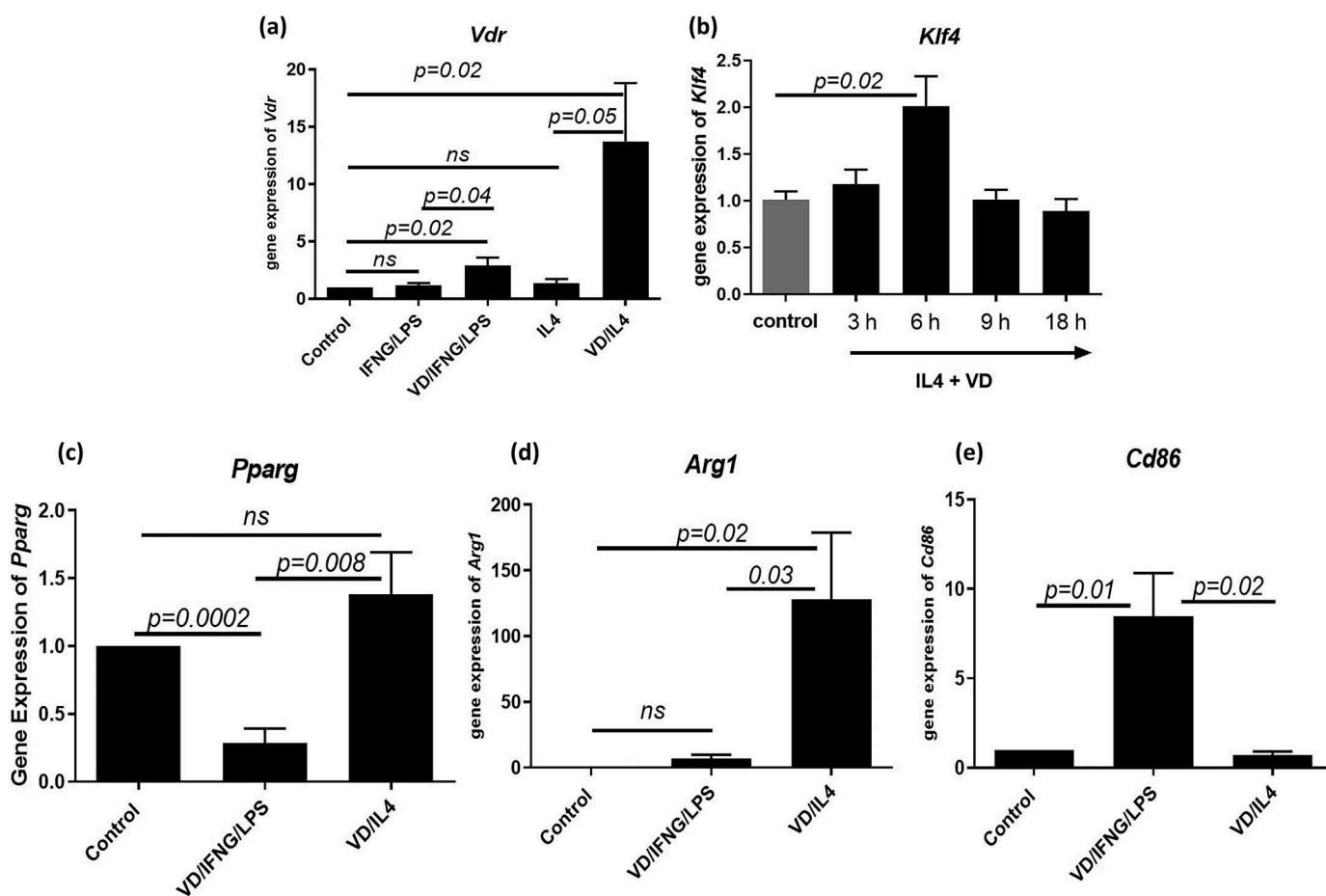
Figure 8. Vitamin D-enhanced autophagy promotes macrophage polarization via activation of KLF4-PPARG pathway. Bone marrow derived macrophages were treated with 1,25 dihydroxy-vitamin D$_3$ (VD)+IL4 or VD+LPS+IFNG for 3 to 24 h as indicated to assess for molecular markers that map the autophagy pathway and M2 macrophage polarization. Gene expression was assessed for (a) Klf4 at 3, 6, 9 and 18 h and (b–e) for 24 h for (b) Vdr, (c) Pparg and (d) Arg1 and (e) Cd86 (n = 4), p<0.05.

vitamin D intervention following sunburn demonstrated increased expression of LC3 in CD163$^+$ macrophages by fluorescence microscopy (Figure 9(a,b) vs (c,d)). Given the fixed small sample size, quantification of cells/HPF demonstrated increased trend but did not achieve statistical significance (Figure S6).

Discussion

Excess exposure to UV radiation contributes to acute skin damage including epidermal injury that initiates an influx of activated immune cells into the wounded skin bed forming a localized inflammatory milieu that further exacerbates inflammation and retards tissue repair [1,18]. Here we show that a single dose of vitamin D dampened inflammation to reduce skin injury following experimentally induced sunburn from UV exposure and was sufficient for cell survival and accelerated tissue recovery. Reduced inflammation was characterized by decreased pro-inflammatory cytokines and culminated in prevention of excessive cellular apoptosis, preservation of histological architecture, and accelerated recovery from a progressive wound. These effects were mediated through vitamin D-enhanced autophagy that support expansion of anti-

inflammatory M2 macrophages and were reversed with inhibition of autophagy. The study also demonstrated that vitamin D treatment facilitated an increase in M2:M1 macrophage ratio to tip the balance towards attenuated inflammation, a delicate balance that is disrupted when the UV inflammation model was recapitulated in myeloid atg7 cKO mice. Finally, our in vitro studies begin to delineate a mechanism by which vitamin D mediates resolution of UV-induced injury through activation of the KLF4-PPARG pathway.

The skin has evolutionarily fortified itself with multiple protective mechanisms in order to prevent DNA and protein damage from exposure to UV rays of sunlight. Since autophagy is a cellular process to remove damaged proteins and organelles, it is possible that autophagy is a tool that has evolved to perform critical homeostatic functions in the skin to regulate a balance between UV rays promoting synthesis of vitamin D and excess UV causing rampant DNA damage [19]. Autophagy is itself regulated by numerous stimuli including starvation, genotoxic and inflammatory stress [8,20] in which disruption of autophagy or deficiency in autophagy genes contributes to a wide variety of disease pathologies including chronic inflammation, tumor progression and cancer [21,22]. The occurrence of uncontrolled cell death from excessive UV
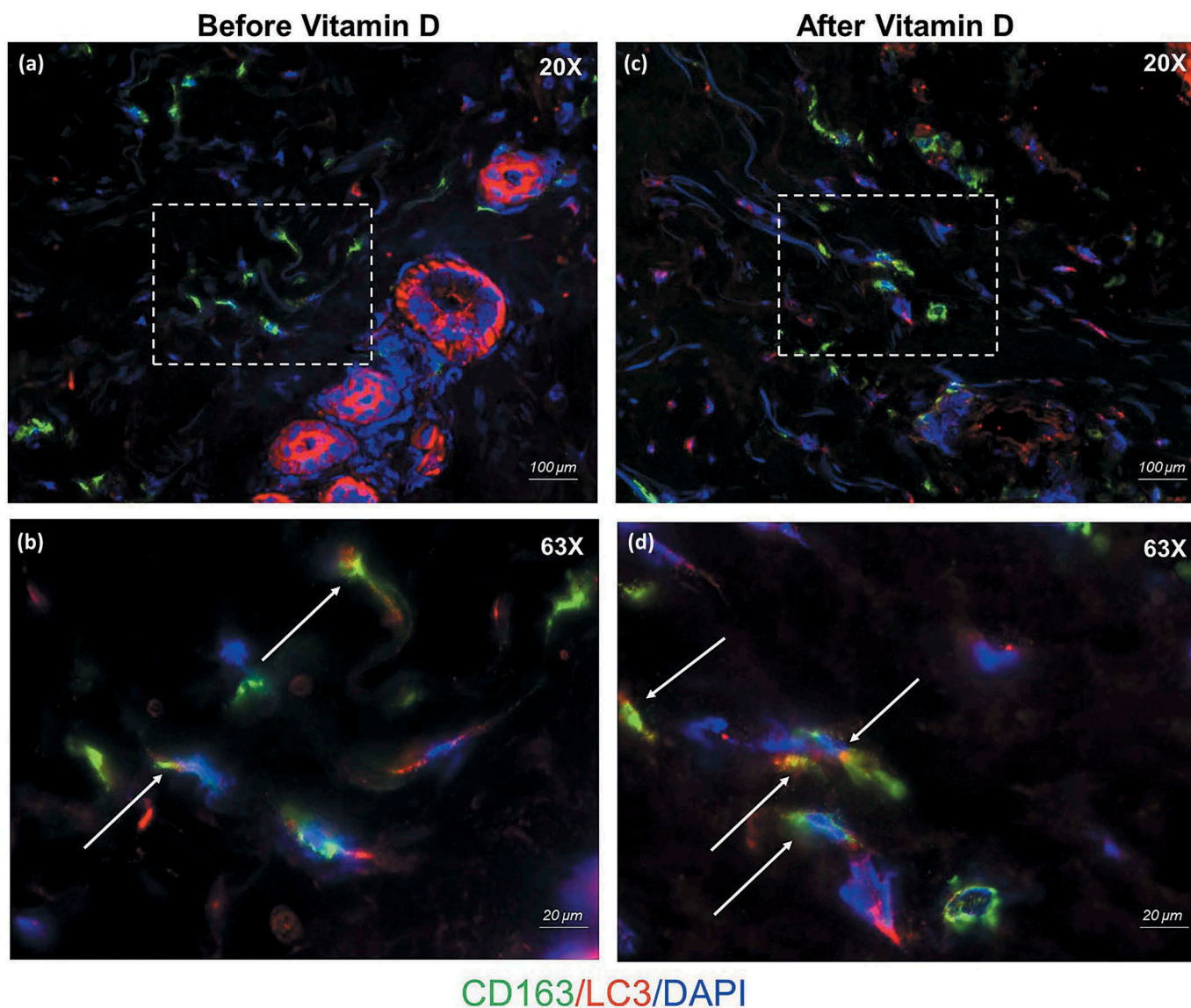
Before Vitamin D   **After Vitamin D**

CD163/LC3/DAPI

Figure 9. Vitamin D (D3) protection from UV-mediated acute inflammation is associated with enhanced macrophage specific autophagy in human skin. Healthy subjects were treated with a single dose of 200,000 IU D3 following exposure to experimentally induced sunburn. Immunofluorescence microscopy detects for the presence of macrophage marker CD163 (green), autophagy marker LC3 (red), and DAPI (blue) from skin biopsies obtained before (a, b) and after (c, d) D3 treatment. Arrows indicate co-localization (yellow). The dotted box in a and c indicate the areas that have been magnified in b and d. Scale bar: 100 μm for 20X magnification and 20 μm for 63X.

exposure is offset by survival signals from upregulated autophagy to augment cellular homeostasis and proliferation [23]. In addition to its critical role in disease pathology, autophagy has emerged as a potent immune regulator to counteract infection and respond to Toll-like receptor signaling to influence cells towards apoptosis or survival [24–26]. Moreover, augmenting autophagy especially in macrophages has been shown to protect from acute and chronic organ injury through attenuation of inflammation, promoting cell survival and by supporting tissue remodeling [27–30]. Enhanced autophagy is shown to protect against polymicrobial sepsis by promoting cell survival, preventing organ damage and dampening cytokine storm triggered by microbial load [31]. These and other studies support the idea that the outcome of enhanced autophagy is largely influenced by the surrounding microenvironment, stress response, disease pathology [32].

Our findings that UV exposure provoked a stress response to induce autophagy resulting in massive apoptosis is consistent with these studies in that intervention with vitamin D and its presence within the cellular microenvironment modified UV-induced autophagy to promoted cell survival and protect against UV-mediated skin damage.

In our model, UV-induced skin inflammation resulted in local tissue injury that supports the preferential expansion of M1 macrophages leading to production of inflammatory cytokines that propagate inflammation, exacerbate the wound, and mediate apoptosis [33,34]. Although the immunomodulatory effect of vitamin D through M2 macrophage polarization has been demonstrated in *in vitro* studies and in disease models of chronic inflammation [11,35,36], we are the first to show that vitamin D enhanced autophagy promotes an appropriate M2 to M1 ratio at the site of inflammation that dampens acute

inflammation and facilitates skin recovery. In contrast to our model of acute inflammation, other studies report that elevated levels of autophagy negatively impacts wound healing in models of chronic inflammation such as in diabetic mice, through preferential expansion of M1 macrophages that propagate inflammation [36–38]. This again reinforces the impact of the cellular environment on the functional outcome of elevated autophagy and therefore can be identified as a potential therapeutic target for future translational studies.

Findings from our recent clinical study on experimentally induced sunburn in human subjects strongly suggest a role for ARG1 in vitamin D mediated reduction of skin inflammation. Our data in the mouse model was consistent with the human study as ARG1 colocalized with MRC1, as was observed in the human samples where ARG1 colocalized with CD163. M2 macrophages synthesize ARG1 to compete with NOS2, induced under inflammation to convert substrate the arginine to ornithine instead of reactive nitric oxide [39]. The evidence that vitamin D decreases NOS2 production and that NOS2 and autophagy operate in an antagonistic manner support the rationale that vitamin D mediated immunomodulation involves autophagy [13,40]. Data obtained from our *atg7* cKO mouse studies contributed to this hypothesis and establishes a novel link between autophagy and vitamin D mediated tissue repair.

Data from other studies using siRNA and antagonists establish a positive link between VDR signaling and M2 polarization via activation of *Pparg*, also an M2-polarizing nuclear receptor [17,35,41]. Attempts to decipher a mechanism for vitamin D regulation of autophagy demonstrates that vitamin D promotes upregulation of M2 transcriptional regulator *Klf4*, M2-priming gene *Pparg* and M2 macrophage marker *Arg1*. Finally, recent studies demonstrating that KLF4 expression is linked to autophagy to promote survival and delay in aging of human skeletal muscle is consistent with our study findings [7]. Taken together, vitamin D-enhanced autophagy can be potentially utilized in diverse clinical settings in which injury induces rapid cell death in tissues and organs by targeting and attenuating hyper-inflammatory responses.

Materials and methods

Mice

Six to 8-week-old pathogen-free female C57BL/6J mice were purchased from Jackson Laboratories. All animals received standard laboratory diet. All animal studies have been approved by Case Western Reserve Institutional Animal Care and Committee. *atg7*^{flox/flox} mice were a gift from Dr. Akiko Maeda, Visual Research Science Center, Case Western Reserve University and *Lyz2/LysM Cre* mice were purchased from Jackson Laboratory. *atg7*^{flox/flox} mice were crossed with *Lyz2/LysM Cre* mice to obtain myeloid-specific *Atg7*-deficient (*Lyz2/LysM Cre Atg7*^{fl/fl}, designated *atg7* cKO) mice and both male and female mice were used for experiments. Genotyping was performed on tail genomic DNA by established methods. *atg7*^{flox/flox} littermates were used as littermate controls. After shaving and chemical depilation of hair from the dorsal skin, mice were allowed to rest for 48 hours before initiation of experiments.

UV radiation, vitamin D and 3-MA treatment

Mice were exposed to UV radiation as described previously [14]. Briefly, a 2 cm2 area of back skin depilated of hair was exposed to UVB irradiation from six FS-40 fluorescent lamps filtered through Kodacel (Eastman Kodak Co., Rochester, NY). UVB emission was measured with an IL-443 phototherapy radiometer (International Light, Newburyport, MA) furnished with an IL SED 240 detector. Mice were exposed to a single UVB dose of 100 mJ/cm2 to induce skin inflammation. Vitamin D (25(OH) D) (Sigma-Aldrich, H4014-1MG) was reconstituted in ethanol (Sigma-Aldrich, E7023-500ML) and diluted in mineral oil (Sigma-Aldrich, M8410) for intraperitoneal injections at 5 ng of vitamin D, 1 h following UV exposure. Where indicated 3-methyl adenine (3-MA) (Sigma-Aldrich, M9281-100MG) at 30 mg/kg was reconstituted in 1X PBS (NaCl, KCl, Na2HPO4, and KH2PO4) for three consecutive intraperitoneal injections on days −2, −1 and 0 relative to UV exposure.

Measurement of area of erythema and wound

The dorsal shaved back of mice were imaged and wounds (area of redness) were measured using Image JTM software and normalizing to a common 1 mm by 1 mm grid on which the mice were recumbent.

Bone marrow derived macrophages

BMDMs were differentiated by L929 conditioned media as previously described [42]. Briefly, cells were re-plated, cultured with RPMI (Thermo Fisher Scientific, 11875085) containing 10% FCS (Thermo Fisher Scientific, 10082147) and stimulated with various agents for 6 h or 24 h to assess for gene expression of molecular determinants of autophagy and inflammation. At the indicated times BMDMs were stimulated with LPS (50 ng/ml; Sigma Aldrich, L2630-10MG), IFNG (20 ng/ml; R&D Systems, 485-MI-100/CF), IL4 (20 ng/ml) (R&D Systems, 404-ML-010/CF), 1,25(OH)2D$_3$ (100 nM; Sigma Aldrich, D1530-10UG).

RNA extraction and quantitative PCR

qPCR was performed as previously described [43]. Mouse skin samples and BMDMs were homogenized using TRIzol reagent (Thermo Fisher Scientific, 15596026) to extract total RNA according to the manufacturer's instructions and quantified using the NanoDrop 2000 (Thermo Scientific, Carlsbad, CA, USA). RNA (100 ng) was required for reverse transcriptase–PCR analysis using TaqMan Gene Expression Assays and the Taqman RNA-to-CT 1-Step kit (Thermo Fisher Scientific, 4392938) for quantification of *Tnf, Nos2, Mmp9, Pparg, Vdr, Arg1, Cd86* (Thermo Fisher Scientific, Mm99999068_m1, Mm01309902_m1, Mm00442991_m1, Mm01184322_m1, Mm00437297_m1, Mm00475988_m1, Mm00444543_m1), *Klf4* (Integrated DNA Technologies, 187934787, 187934788) mRNA expression. Samples were analyzed using a Step-One System (Applied Biosystems, Grand Island, NY) based on manufacturer's recommendations. Gene expression was expressed as fold changes normalized to the 18S (Thermo Fisher Scientific, Hs99999901_s1) RNA housekeeping gene.

Human Skin Specimens

OCT-embedded human skin sections 8-μm thick were obtained from our previously published trial approved by The Institutional Review Board at University Hospitals Cleveland Medical Center. The trial is registered with clinical-trials.gov(NCT02920502).

Western blots

Frozen skin tissue was homogenized by mechanical bead beating and protein lysates prepared using Pierce RIPA buffer (Thermo Fisher Scientific, 89900) containing protease and phosphatase inhibitors (Thermo Fisher Scientific, 1861280). Samples were quantitated using Pierce BCA Protein Assay Kit (Thermo Fisher Scientific, 23225). Samples were prepared under reducing conditions and run on a 4–12% bis tris gradient gel (Thermo Fisher Scientific, NW04122BOX) using the manufacturer's recommended protocol. Proteins were transferred onto a 0.2-μm PVDF membrane (Thermo Fisher Scientific, LC2002). Membrane was blocked with 5% non-fat milk, 1% BSA (Sigma Aldrich, 05470), and 10% chicken serum (Sigma Aldrich, C5405) in 1x TBS-T (Sigma Aldrich, 91414). Anti-LC3 (Novus Biologicals, NB100-2220), anti-SQSTM1 (BD Biosciemces, 610833) and anti-GAPDH (Santa Cruz Biotechnology, sc-25778) were used for detection of target proteins with an anti-IgG HRP conjugated secondary antibody (Santa Cruz Biotechnology, sc-2955). Development of protein signal was achieved using SuperSignal West Pico PLUS substrate (Thermo Fisher Scientific, 34580). Immunoblots were quantified by densitometry.

H&E staining

UV irradiated and control skin from euthanized mice were removed and fixed in 10% formalin diluted in PBS (Fisher Scientific, 23 245684). Samples were then embedded in paraffin, sectioned (8-μm thickness), stained with H&E to evaluate UV-induced inflammation, cellular infiltration, and skin damage.

TUNEL assay

The TUNEL assay was performed on slide mounted mouse skin tissue sections using the In situ Cell Death Detection kit, (Roche Applied Science, 11684809910) according to the manufacturer's directions and visualized using a Leica DMI 6000 B inverted fluorescent microscope (Leica Microsystems Wetzlar, Germany) using a Retiga Aqua blue camera (Q-imaging Vancouver British Columbia).

Immunocytometry

Control and UV-exposed mouse skin was chopped and digested with Liberase 0.5 mg/ml (Roche Applied Science, 5401020001) for 60 min to release cells. Following digestion, the cells were sequentially filtered through 70- and 40-μm sieves, they were then plated on tissue culture coated cover slips (MatTek Corporation, P35G-0.170-14-C), stained for ADGRE1/F4/80 (eBioscience, 50-167-59) and LC3B (Novus Biologicals, NB100-2220) and imaged by Leica DMI 6000 B inverted fluorescence microscope (Leica Microsystems Wetzlar, Germany) using a Retiga Aqua blue camera (Q-imaging Vancouver British Columbia).

Immunofluorescence microscopy

OCT-embedded skin tissue was sectioned 8-μm thick and subjected to staining as described before [43]. Primary antibodies used in 10% goat serum (Sigma Aldrich, G9023) are the following: anti-mouse ADGRE1/F4/80 antigen Alexa Fluor 488; rat IgG2a isotype-Alexa Fluor 488 (eBioscience, 50-167-59, NC9879806; 1:50); MAP1LC3B antibody (Novus Biologicals, NB100-2220; 1:500); BV421-MRC1/CD206 (BioLegend, 141717); anti-human CD163 antibody (Bio-Rad, MCA1853; 1:50); mouse IgG1 isotype (Bio-Rad, MCA 928; 1:50). Secondary antibodies: goat anti-rabbit Alexa Fluor 647 (1:2,000 in 1X PBS; Life Technologies, A32733) and goat anti-rabbit Alexa Fluor 488 (1:2,000 in 1X PBS; Life Technologies, A-11034). Samples were stained with DRAQ5 (BioLegend, 424101; 1:1000) and mounted with Fluoromount G (Electron Microscopy Sciences, 17984-25) or mounting media containing DAPI (Abcam, ab104139). Sections were imaged using the Leica DMI 6000 B inverted fluorescence microscope (Leica Microsystems Wetzlar, Germany) using a Retiga Aqua blue camera (Q-imaging Vancouver British Columbia).

Flow cytometry

Mouse skin from UV-exposed and control mice were Liberase digested at 0.5 mg/ml dilution (Roche Applied Science, 5401020,001) to isolate skin cells. Single cell suspension in FACS staining buffer (containing 1% BSA [Thermo Fisher Scientific, 10082147] 5 mM EDTA [Thermo Fisher Scientific, AM9260G]) was subject to staining for cell surface markers APC-Cy7 PTPRC (protein tyrosine phosphatase, receptor type, C) (BD Biosciences, BDB557659), PE ADGRE1/F4/80 (BioLegend, 123110) and APC LY6C/Ly6C (lymphocyte antigen 6 complex, locus C1) (BD Biosciences, 560595). Intracellular markers used to further characterize the cells and indicate autophagy were BV421-MRC1/CD206 (BioLegend, 141717) and Alexa Fluor 488-LC3 (Novus Biologicals, NB600-1384AF488). Cells were fluorescently labeled strategically to eliminate spectral overlap. Flow cytometry analysis was conducted using the FlowJo software (FlowJo, Ashland OR) [44].

Transmission electron microscopy

Mouse skin tissue was excised from skin 48 h post exposure. Tissues were prepared for electron microscopy using a protocol describes previously [45,46]. Tissues were fixed with triple aldehyde-DMSO fixative for 2 h at RT. The specimens were thoroughly rinsed in 0.1 M HEPES buffer, pH 7.4, then post fixed for 2 h in an unbuffered 1:1 mixture of 2% osmium tetroxide and 3% potassium ferricyanide. After rinsing with distilled water, the specimens were soaked overnight in an acidified solution of 0.25% uranyl acetate. After another rinse in distilled water, they were dehydrated in ascending concentrations of ethanol, passed through propylene oxide, and embedded in Poly/Bed resin mixture (Polysciences, 08792–1). Thin sections were sequentially stained with acidified uranyl acetate followed by a modification of Sato's triple lead stain and examined in a FEI Tecnai Spirit (T12) with a Gatan US4000 4kx4k CCD.

Statistical analysis

Significant differences of multiple markers between groups of mice were determined using a Students t-test. Outliers were excluded based on Routs statistical analysis.

Competing financial interests

The authors declare no competing interests.

Disclosure statement

No potential conflict of interest was reported by the authors.

ORCID

Kurt Q. Lu http://orcid.org/0000-0002-8297-433X

References

[1] Ryser S, Schuppli M, Gauthier B, et al. UVB-induced skin inflammation and cutaneous tissue injury is dependent on the MHC class I-like protein, CD1d. J Invest Dermatol. 2014;134 (1):192–202.

[2] Young AR. Acute effects of UVR on human eyes and skin. Prog Biophys Mol Biol. 2006;92(1):80–85.

[3] Faustin B, Reed JC. Sunburned skin activates inflammasomes. Trends Cell Biol. 2008;18(1):4–8.

[4] Scott JF, Das LM, Ahsanuddin S, et al. Oral vitamin D rapidly attenuates inflammation from sunburn: an interventional study. J Invest Dermatol. 2017;137:2078–2086.

[5] Høyer-Hansen M, Nordbrandt SPS, Jäättelä M. Autophagy as a basis for the health-promoting effects of vitamin D. Trends Mol Med. 2010;16(7):295–302.

[6] Helming L, Böse J, Ehrchen J, et al. 1alpha,25-Dihydroxyvitamin D3 is a potent suppressor of interferon gamma-mediated macrophage activation. Blood. 2005;106(13):4351–4358.

[7] Hsieh PN, Zhou G, Yuan Y, et al. A conserved KLF-autophagy pathway modulates nematode lifespan and mammalian age-associated vascular dysfunction. Nat Commun. 2017;8(1):914.

[8] Chen RJ, Lee YH, Yeh YL, et al. The roles of autophagy and the inflammasome during environmental stress-triggered skin inflammation. Int J Mol Sci. 2016;17(12):2063.

[9] Mahil SK, Twelves S, Farkas K, et al. AP1S3 mutations cause skin autoinflammation by disrupting keratinocyte autophagy and up-regulating IL-36 production. J Invest Dermatol. 2016;136 (11):2251–2259.

[10] Liu K, Zhao E, Ilyas G, et al. Impaired macrophage autophagy increases the immune response in obese mice by promoting proinflammatory macrophage polarization. Autophagy. 2015;11 (2):271–284.

[11] Zhang X-L, Guo Y-F, Song Z-X, et al. Vitamin D prevents podocyte injury via regulation of macrophage M1/M2 phenotype in diabetic nephropathy rats. Endocrinology. 2014;155(12):4939–4950.

[12] Yang Z, Ming XF. Functions of arginase isoforms in macrophage inflammatory responses: impact on cardiovascular diseases and metabolic disorders. Front Immunol. 2014;5:533.

[13] Sarkar S, Korolchuk VI, Renna M, et al. Complex inhibitory effects of nitric oxide on autophagy. Mol Cell. 2011;43(1):19–32.

[14] Toichi E, Lu KQ, Swick AR, et al. Skin-infiltrating monocytes/macrophages migrate to draining lymph nodes and produce IL-10 after contact sensitizer exposure to UV-irradiated skin. J Invest Dermatol. 2008;128(11):2705–2715.

[15] Cooper KD, Duraiswamy N, Hammerberg C, et al. Neutrophils, differentiated macrophages, and monocyte/macrophage antigen presenting cells infiltrate murine epidermis after UV injury. J Invest Dermatol. 1993;101(2):155–163.

[16] Khoury-Hanold W, Iwasaki A. Autophagy snuffs a macrophage's inner fire. Cell Host Microbe. 2016;19(1):9–11.

[17] Liao X, Sharma N, Kapadia F, et al. Kruppel-like factor 4 regulates macrophage polarization. J Clin Invest. 2011;121(7):2736–2749.

[18] Clydesdale GJ, Dandie GW, Muller HK. Ultraviolet light induced injury: immunological and inflammatory effects. Immunol Cell Biol. 2001;79(6):547–568.

[19] Qiang L, Zhao B, Shah P, et al. Autophagy positively regulates DNA damage recognition by nucleotide excision repair. Autophagy. 2016;12(2):357–368.

[20] Song S, Tan J, Miao Y, et al. Crosstalk of autophagy and apoptosis: involvement of the dual role of autophagy under ER stress. J Cell Physiol. 2017;232:2977–2984.

[21] Peng Y, Miao H, Wu S, et al. ABHD5 interacts with BECN1 to regulate autophagy and tumorigenesis of colon cancer independent of PNPLA2. Autophagy. 2016;12(11):2167–2182.

[22] Virgin HW, Levine B. Autophagy genes in immunity. Nat Immunol. 2009;10(5):461–470.

[23] Strozyk E, Kulms D. The role of AKT/mTOR pathway in stress response to UV-irradiation: implication in skin carcinogenesis by regulation of apoptosis, autophagy and senescence. Int J Mol Sci. 2013;14(8):15260–15285.

[24] Munz C. Enhancing immunity through autophagy. Annu Rev Immunol. 2009;27:423–449.

[25] Levine B, Deretic V. Unveiling the roles of autophagy in innate and adaptive immunity. Nat Rev Immunol. 2007;7(10):767–777.

[26] Chung KM, Yu SW. Interplay between autophagy and programmed cell death in mammalian neural stem cells. BMB Rep. 2013;46(8):383–390.

[27] Han J, Bae J, Choi C-Y, et al. Autophagy induced by AXL receptor tyrosine kinase alleviates acute liver injury via inhibition of NLRP3 inflammasome activation in mice. Autophagy. 2016;12 (12):2326–2343.

[28] Hu Y, Lou J, Mao -Y-Y, et al. Activation of MTOR in pulmonary epithelium promotes LPS-induced acute lung injury. Autophagy. 2016;12(12):2286–2299.

[29] Li H, Peng X, Wang Y, et al. Atg5-mediated autophagy deficiency in proximal tubules promotes cell cycle G2/M arrest and renal fibrosis. Autophagy. 2016;12(9):1472–1486.

[30] Liu WJ, Luo M-N, Tan J, et al. Autophagy activation reduces renal tubular injury induced by urinary proteins. Autophagy. 2014;10 (2):243–256.

[31] Jiang Y, Gao M, Wang W, et al. Sinomenine hydrochloride protects against polymicrobial sepsis via autophagy. Int J Mol Sci. 2015;16(2):2559–2573.

[32] Choi AM, Ryter SW, Levine B. Autophagy in human health and disease. N Engl J Med. 2013;368(7):651–662.

[33] Koh TJ, DiPietro LA. Inflammation and wound healing: the role of the macrophage. Expert Rev Mol Med. 2011;13:e23.

[34] Qiang L, Wu C, Ming M, et al. Autophagy controls p38 activation to promote cell survival under genotoxic stress. J Biol Chem. 2013;288(3):1603–1611.

[35] Jin B, Zhou X, Li B, et al. 1,25-Dihydroxyvitamin D(3) Promotes High Glucose-Induced M1 Macrophage Switching to M2 via the VDR-PPARgamma Signaling Pathway. Biomed Res Int. 2015;2015:157834.

[36] Wang Y, Li Y-B, Yin -J-J, et al. Autophagy regulates inflammation following oxidative injury in diabetes. Autophagy. 2013;9(3):272–277.

[37] Hoyer-Hansen M, Jaattela M. AMP-activated protein kinase: a universal regulator of autophagy? Autophagy. 2007;3(4):381–383.

[38] Guo Y, Lin C, Xu P, et al. AGEs induced autophagy impairs cutaneous wound healing via stimulating macrophage polarization to M1 in diabetes. Sci Rep. 2016;6:36416.

[39] Rath M, Müller I, Kropf P, et al. Metabolism via arginase or nitric oxide synthase: two competing arginine pathways in macrophages. Front Immunol. 2014;5:532.

[40] Au L, Meisch JP, Das LM, et al. Suppression of hyperactive immune responses protects against nitrogen mustard injury. J Invest Dermatol. 2015;135(12):2971–2981.

[41] Bouhlel MA, Derudas B, Rigamonti E, et al. PPARgamma activation primes human monocytes into alternative M2 macrophages with anti-inflammatory properties. Cell Metab. 2007;6(2):137–143.

[42] Riches DW, Henson PM, Remigio LK, et al. Differential regulation of gene expression during macrophage activation with a polyribonucleotide. The role of endogenously derived IFN. J Immunol. 1988;141(1):180–188.

[43] Das LM, Rosenjack J, Au L, et al. Hyper-inflammation and skin destruction mediated by rosiglitazone activation of macrophages in IL-6 deficiency. J Invest Dermatol. 2015;135 (2):389–399.

[44] Rose S, Misharin A, Perlman H. A novel Ly6C/Ly6G-based strategy to analyze the mouse splenic myeloid compartment. Cytometry A. 2012;81(4):343–350.

[45] Fujioka H, Tandler B, Cohen M, et al. Multiple mitochondrial alterations in a case of myopathy. Ultrastruct Pathol. 2014;38 (3):204–210.

[46] Fujioka H, Tandler B, Rosca M, et al. Multiple muscle cell alterations in a case of encephalomyopathy. Ultrastruct Pathol. 2014;38(1):13–25.